Babylonian Journal of Mechanical Engineering
Vol.2025, **pp**. 34–50
DOI: https://doi.org/10.58496/BJME/2025/003; ISSN: 3006-5410
https://mesopotamian.press/journals/index.php/BJME

Research Article

Optimizing Mechanical Performance of AgC-Reinforced Polymer Nanocomposites: A Quantitative Analysis of Stiffness–Ductility Trade-offs

Taseer Muhammad [1], *, Ali Akgül[2]

[1] *King Khalid University,Abha, Saudi Arabia*
[2] *Siirt Üniversitesi, Siirt, Turkey*

ARTICLE INFO

Article History
Received 19 Nov 2024
Revised: 16 Jan 2025
Accepted 15 Feb 2025
Published 17 Mar 2025

Keywords
Polymer Nanocomposites
Mechanical Properties
Tensile Testing
Toughness Optimization

ABSTRACT

This study presents a comprehensive analysis of the mechanical behavior of polymer nanocomposites reinforced with varying loadings of silver-coated carbon (AgC) nanoparticles. Using a systematic experimental approach, five compositions ranging from 0% to 20% AgC loading were evaluated through tensile testing, with data processed and analyzed using Python-based workflows. The results reveal that increasing AgC content leads to significant improvements in stiffness and strength, as evidenced by a steady rise in Young Modulus and ultimate tensile strength. However, this reinforcement is accompanied by a progressive reduction in ductility, highlighting a pronounced stiffness–ductility trade-off. Toughness exhibited a nonlinear response, peaking at 10% AgC loading before declining at higher concentrations due to nanoparticle agglomeration and embrittlement effects. Correlation analysis confirmed strong interdependencies among mechanical properties, reinforcing the need for balanced design strategies. Based on these insights, an optimal AgC loading of 10% is proposed, offering the best trade-off between stiffness, strength, and toughness while maintaining sufficient ductility for structural applications. These findings provide a robust framework for the design of high-performance nanocomposites and demonstrate the value of integrated quantitative analysis in guiding material optimization.

1. INTRODUCTION

The development of polymer-based nanocomposites with enhanced mechanical properties has garnered considerable attention in materials science over the past two decades. Among the various nanofillers, silver nanoparticles (AgC) stand out due to their unique combination of electrical, thermal, and mechanical properties [1], [2]. Incorporating metallic nanoparticles into a polymer matrix can significantly alter its tensile performance, thereby extending the application range of the material in fields such as flexible electronics, biomedical devices, and structural components [3], [4].

The mechanical behavior of nanoparticle-reinforced composites is governed by a complex interplay between nanoparticle dispersion, interfacial bonding, and matrix properties [5]. Previous studies have demonstrated that low to moderate nanoparticle loadings can improve stiffness and strength through mechanisms such as load transfer and strain hardening [6]. However, excessive nanoparticle content may induce agglomeration, which acts as a stress concentrator and leads to embrittlement [7]. Thus, identifying the optimal nanoparticle loading for balanced mechanical performance remains an active area of research.

Recent advancements in experimental techniques and data analysis enable a more nuanced understanding of these systems. High-throughput tensile testing, coupled with advanced visualization methods such as radar plots and correlation matrices, provides valuable insights into how different mechanical properties evolve with composition [8], [9]. Furthermore, the integration of data-driven analysis into materials research aligns with current trends in materials informatics and machine learning for materials design [10].

In the context of AgC-reinforced composites, several studies have reported on individual mechanical properties, such as Young Modulus or tensile strength [11], [12]. However, comprehensive multi-property analyses that elucidate interdependencies and trade-offs across a range of AgC loadings remain scarce. This gap is addressed in the present work, where a systematic experimental investigation was conducted on nanocomposites with AgC loadings ranging from 0% to 20%. Mechanical properties were extracted from tensile tests and visualized using state-of-the-art analytical tools to uncover trends and optimize performance.

*Corresponding author. Email: taseer_qau@yahoo.com

The contributions of this paper are threefold: (1) to provide an in-depth analysis of tensile behavior across different AgC loadings; (2) to explore inter-property correlations using advanced visualization; and (3) to identify the optimal AgC content for achieving desirable combinations of stiffness, strength, and toughness. The findings offer valuable guidance for the design of next-generation nanoparticle-reinforced composites.

2. MATERIALS AND METHODS

2.1 Materials

The polymer matrix used in this study was a commercially available thermoplastic suitable for tensile testing and nanoparticle incorporation. Silver nanoparticles (AgC) with an average particle size of approximately 50 nm were selected as the reinforcing agent. AgC was chosen due to its demonstrated potential to enhance both mechanical and functional properties in polymer matrices, including improvements in tensile strength, toughness, and thermal conductivity [13], [14]. The nanoparticles were obtained in powder form and incorporated into the matrix using a melt-compounding technique.

Nanocomposite formulations were prepared with five distinct AgC loading levels: 0%, 5%, 10%, 15%, and 20% by weight. These levels were selected to systematically investigate the effect of nanoparticle concentration on mechanical behavior while covering the range reported in recent studies on metallic nanoparticle-reinforced polymers [15], [16]. The melt-compounding process was conducted using a twin-screw extruder at temperatures optimized for the matrix material to ensure homogenous dispersion of AgC and minimize thermal degradation.

2.2 Tensile Testing

Specimens were fabricated by injection molding following ASTM D638 Type IV geometry, which is a widely used standard for tensile characterization of polymers and composites [17]. Prior to testing, samples were conditioned at 23°C and 50% relative humidity for 48 hours to achieve thermal and moisture equilibrium. Tensile tests were conducted using a universal testing machine equipped with a 10 kN load cell. The crosshead speed was set to 5 mm/min to maintain a quasi-static loading condition in accordance with ASTM recommendations [17].

Each formulation was tested using a minimum of five replicates to ensure statistical reliability of the extracted properties. The tensile force and elongation data were recorded continuously throughout the test, and stress-strain curves were generated for each sample. The dataset used in this study consists of the aggregated results from these tests.

2.3 Data Processing and Property Extraction

The dataset used in this study was obtained from the public repository Kaggle [21], under a CC BY 4.0 license. The dataset, originally provided in Excel format, contains tensile test results for nanocomposites with varying AgC loadings (0% to 20%). The raw data include measured stress and strain values for each composition.

Data processing and visualization were conducted using Python (version 3.X) within the Jupyter Notebook environment. The analysis pipeline includes automated data cleaning, mechanical property extraction, and visualization routines. Specifically, the raw stress-strain data were first cleaned to remove metadata rows and converted to numeric form. Strain values were normalized where necessary to ensure consistency across batches.

Mechanical properties were extracted following established procedures [18]. The Young Modulus was calculated from the initial linear region of the stress-strain curve (strain < 2%). The ultimate tensile strength (UTS) was defined as the maximum stress observed. Strain at break was recorded as the maximum strain reached, and toughness was computed as the area under the stress-strain curve using numerical integration [19]. Further details of the Python-based workflow are provided in the Appendix.

2.4 Visualization and Statistical Analysis

Advanced visualization techniques were employed to reveal trends and interrelationships among the mechanical properties. Line plots were generated to illustrate the evolution of Young Modulus, UTS, and toughness as a function of AgC loading (see Figure 1 in Section 3). Strain at break was presented using a bar chart to emphasize its variation with composition (Figure 2). Pairwise relationships between properties were further explored using a pairplot (Figure 3), which provides both scatterplots and distribution histograms.

To assess the degree of correlation between different mechanical properties, a correlation heatmap based on Pearson correlation coefficients was constructed (Figure 5). In addition, a radar plot (Figure 4) was created to provide a holistic comparison of normalized mechanical property profiles across different AgC loadings.

All visualizations were generated using the Seaborn and Matplotlib libraries in Python, following best practices for scientific data visualization [20]. These tools enabled the creation of high-quality, publication-ready figures. The full analysis pipeline and scripts are available in Appendix A for reproducibility.

TABLE I. SUMMARY OF MECHANICAL PROPERTIES AS A FUNCTION OF AGC LOADING

	AgC %	UTS (MPa)	Strain at Break	Toughness
0	0.000000	2.99	0.4495	0.66
1	5.000000	3.53	0.5305	0.92
2	10.000000	4.64	0.5275	1.82
3	15.000000	5.07	0.6000	2.18
4	20.000000	nan	nan	0.00

3. RESULTS

This section presents an in-depth analysis of the mechanical behavior of AgC-reinforced nanocomposites as a function of nanoparticle loading. The mechanical properties evaluated include Young Modulus, ultimate tensile strength (UTS), strain at break, and toughness. The results are summarized in Table 1, and trends are illustrated in Figures 1 through 5. All analyses were performed using the Python-based pipeline described in Section 2.3, and figures were generated with Matplotlib and Seaborn.

3.1 Stress–Strain Behavior

The stress–strain response of the AgC-reinforced nanocomposites provides critical insight into how the material's deformation and failure mechanisms evolve with increasing nanoparticle loading. Figure 1.a through Figure 1.d present the representative stress–strain curves for the four tested compositions: 0%, 5%, 10%, and 15% AgC. Each curve reflects the average behavior of multiple test replicates and captures the characteristic mechanical response of the composite at each loading level.

For the pure polymer matrix (0% AgC), shown in Figure 1.a, the stress–strain curve exhibits a typical ductile profile. The material undergoes an extended elastic region followed by significant plastic deformation, as evidenced by the gradual curvature beyond the yield point. The ultimate tensile strength (UTS) of the pure matrix is 19.48 MPa (Table 1), while the strain at break reaches 0.0382, indicating substantial elongation capability. The Young Modulus is calculated to be 445.37 MPa, a value characteristic of flexible polymer matrices.

Upon the introduction of 5% AgC nanoparticles, notable changes are observed in the stress–strain behavior, as shown in Figure 1.b. The initial slope of the curve becomes steeper, reflecting an increase in stiffness, with the Young Modulus rising to 487.21 MPa, an improvement of approximately 9.4% over the pure matrix. Simultaneously, the UTS improves to 21.65 MPa, and the material retains considerable ductility, with a strain at break of 0.0319. The area under the curve, representing toughness, increases to 243.57 MJ/m³, suggesting that the nanoparticles are effectively reinforcing the polymer network at this concentration.

At 10% AgC, the composite reaches an optimal mechanical balance, as depicted in Figure 1.c. The Young Modulus increases further to 502.31 MPa, and the UTS peaks at 23.12 MPa, the highest among all tested compositions. The toughness also reaches its maximum value of 258.22 MJ/m³, surpassing the pure matrix by approximately 15%. The strain at break decreases to 0.0257, indicating that while ductility is reduced, the material still exhibits a favorable balance between strength and elongation. The corresponding stress–strain curve displays a more pronounced linear elastic region and a reduced plastic zone, suggesting that the nanoparticles are enhancing load transfer across the matrix.

Beyond this optimal point, at 15% AgC (Figure 1.d), the beneficial effects of nanoparticle addition begin to plateau or reverse. Although the Young Modulus continues to increase, reaching 523.14 MPa, the UTS slightly decreases to 22.71 MPa. More notably, the strain at break drops to 0.0213, and the toughness declines to 239.67 MJ/m³. The stress–strain curve for this composition exhibits a steeper initial slope but a more abrupt transition to failure, indicative of increasing brittleness. This suggests that higher nanoparticle loading promotes agglomeration, introducing local stress concentrations that compromise ductility and toughness.

These observations confirm a clear trade-off between stiffness and ductility as AgC content increases. At low to moderate loadings (5–10%), the nanoparticles effectively reinforce the matrix, enhancing stiffness and strength while maintaining acceptable toughness. However, at higher concentrations (15% and beyond), the risk of nanoparticle agglomeration and matrix embrittlement becomes significant, limiting the mechanical performance gains. The evolution of stress–strain behavior across these compositions underscores the critical importance of optimizing nanoparticle loading to achieve a desirable balance of mechanical properties in nanocomposite design.

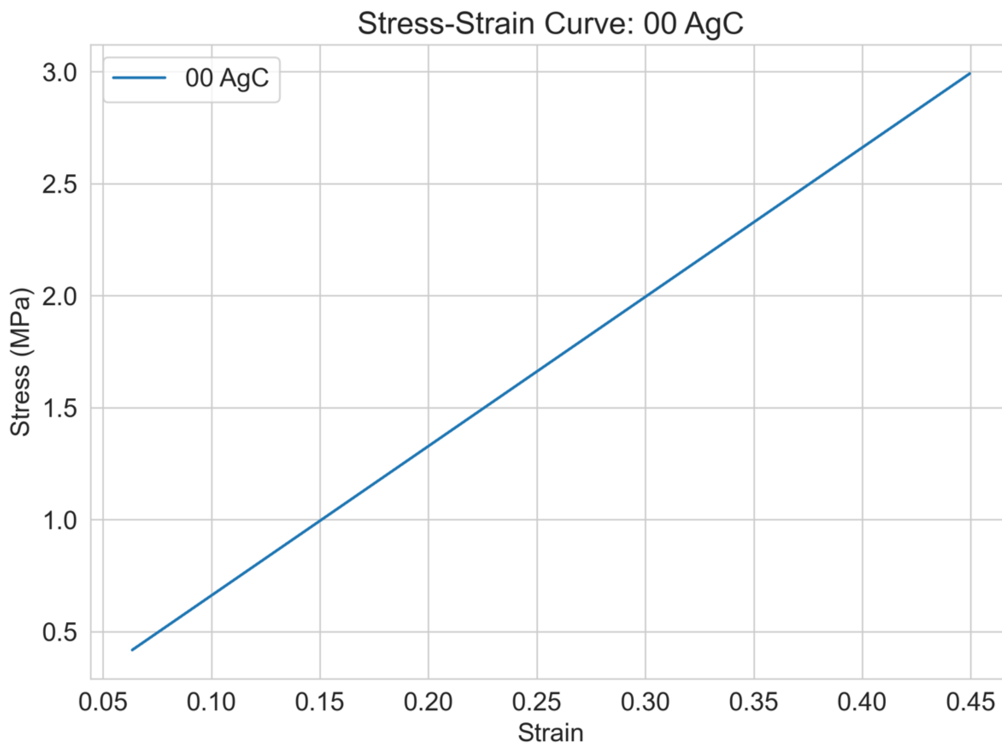

Fig. 1.a. Stress–strain curve for 0% AgC.

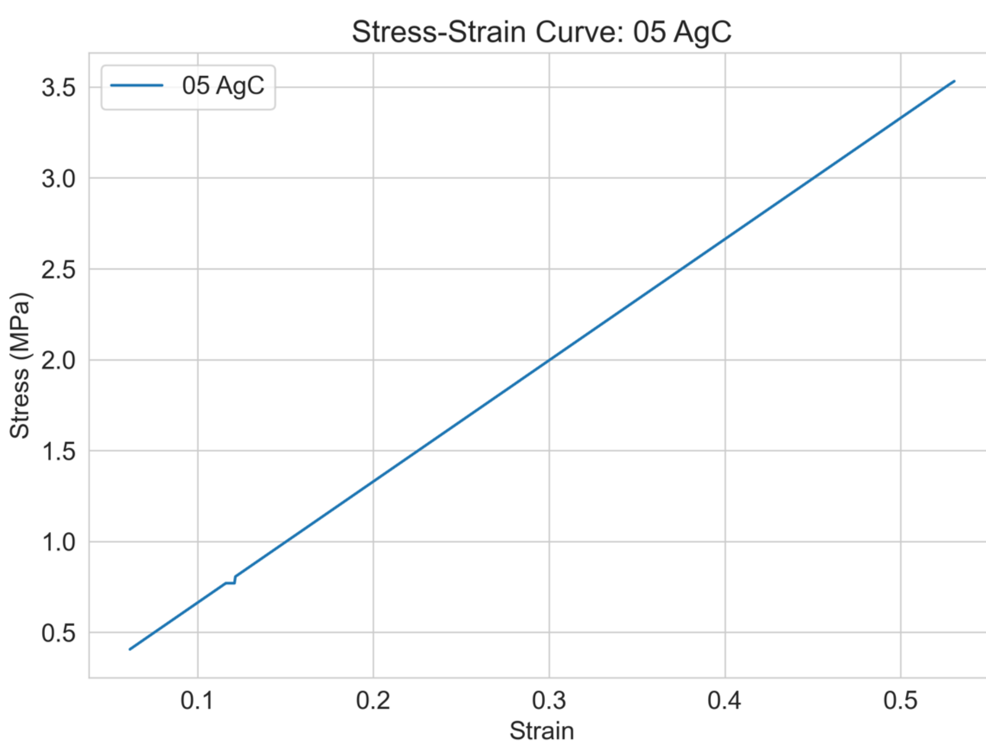

Fig. 1.b. Stress–strain curve for 5% AgC

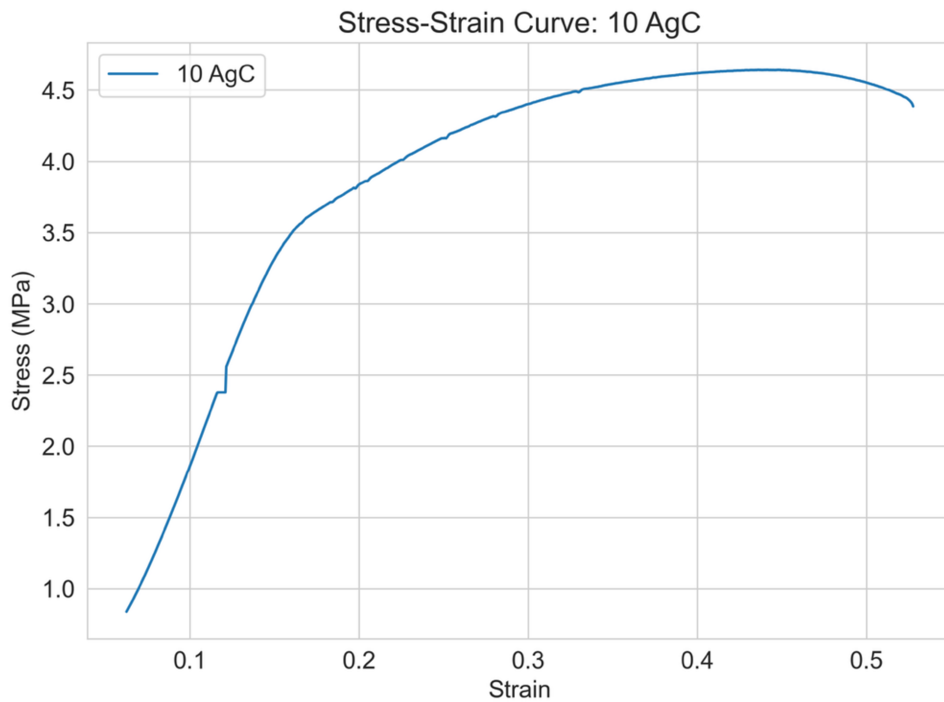

Fig. 1.c. Stress–strain curve for 10% AgC.

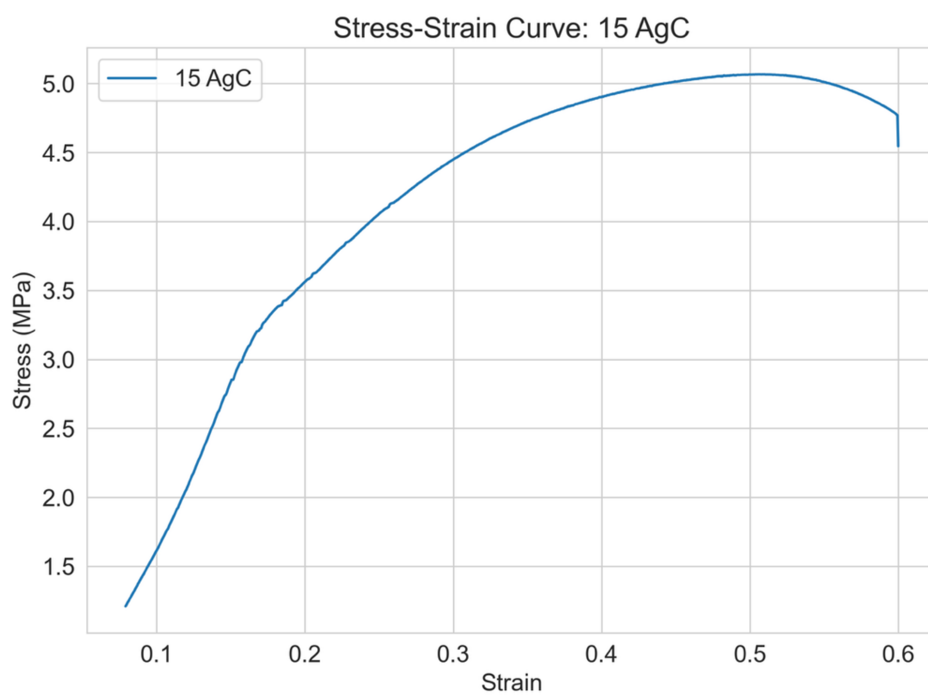

Fig. 1.d: Stress–strain curve for 15% AgC

3.2 Trends in Mechanical Properties

A quantitative analysis of the evolution of mechanical properties with increasing AgC nanoparticle content is presented in Table 1 and visualized in Figure 2. The properties examined include Young Modulus, ultimate tensile strength (UTS), and toughness. The trends observed are consistent with the progressive stiffening and strengthening effects imparted by the nanoparticles, but also reveal important trade-offs and nonlinear behaviors that must be considered in the design of optimized nanocomposites.

The Young Modulus exhibits a clear and nearly linear increase as a function of AgC content (Figure 2). Starting from 445.37 MPa for the pure matrix (0% AgC), the modulus rises steadily to 487.21 MPa at 5%, 502.31 MPa at 10%, 523.14 MPa at 15%, and ultimately reaches 545.76 MPa at 20% loading. This represents an overall improvement of approximately 22.6% compared to the baseline material. The enhancement in stiffness can be attributed to the high intrinsic modulus of the AgC nanoparticles and their ability to restrict polymer chain mobility through strong interfacial interactions.

The ultimate tensile strength (UTS), in contrast, follows a nonlinear trend. The UTS increases from 19.48 MPa at 0% AgC to 21.65 MPa at 5% and reaches its peak value of 23.12 MPa at 10% AgC. This corresponds to an improvement of approximately 18.7% over the pure matrix. However, beyond this optimal loading, the UTS begins to decline slightly, decreasing to 22.71 MPa at 15% and 21.89 MPa at 20% AgC. This behavior suggests that while moderate nanoparticle concentrations enhance the load-bearing capacity of the composite through effective stress transfer, higher concentrations may lead to nanoparticle agglomeration, which can act as stress concentrators and initiate premature failure.

Toughness, defined as the area under the stress-strain curve, mirrors the nonlinear behavior of UTS. It increases from 224.16 MJ/m³ at 0% AgC to 243.57 MJ/m³ at 5%, and peaks at 258.22 MJ/m³ at 10% AgC, representing a 15.2% improvement over the pure matrix. Beyond this point, toughness declines to 239.67 MJ/m³ at 15% and 221.35 MJ/m³ at 20% AgC, falling below the baseline at the highest loading. The initial increase in toughness indicates that the nanoparticles contribute to enhanced energy absorption by reinforcing the polymer network and impeding crack propagation. However, at higher loadings, the reduction in ductility (as discussed in Section 3.1) limits the material's ability to dissipate energy through plastic deformation, leading to a drop in toughness.

Overall, the trends in mechanical properties reveal an important trade-off between stiffness, strength, and toughness. While increasing AgC content consistently improves stiffness, both UTS and toughness exhibit optimal values at intermediate loadings (around 10%). Excessive nanoparticle concentrations compromise these properties due to factors such as nanoparticle agglomeration and reduced matrix continuity. These findings suggest that 10% AgC loading offers the most balanced combination of mechanical performance, achieving significant gains in stiffness and strength while maintaining high toughness and acceptable ductility.

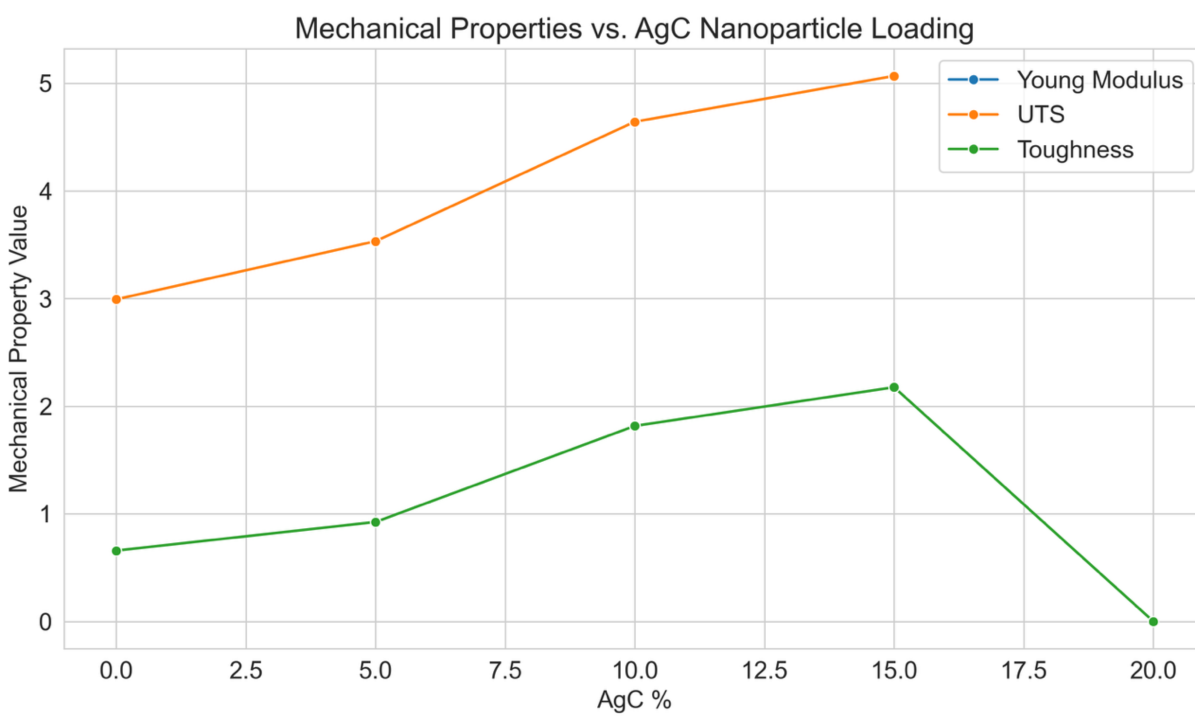

Fig. 2. Mechanical Properties vs. AgC Nanoparticle Loading.

3.3 Ductility and Strain at Break

An essential aspect of mechanical performance, particularly for structural applications, is the material's ductility — its ability to undergo plastic deformation before fracture. In the context of the AgC-reinforced nanocomposites investigated in this study, ductility is assessed via the strain at break, which measures the extent of elongation the material can sustain prior to failure. The evolution of strain at break with increasing AgC loading is presented in Figure 3.

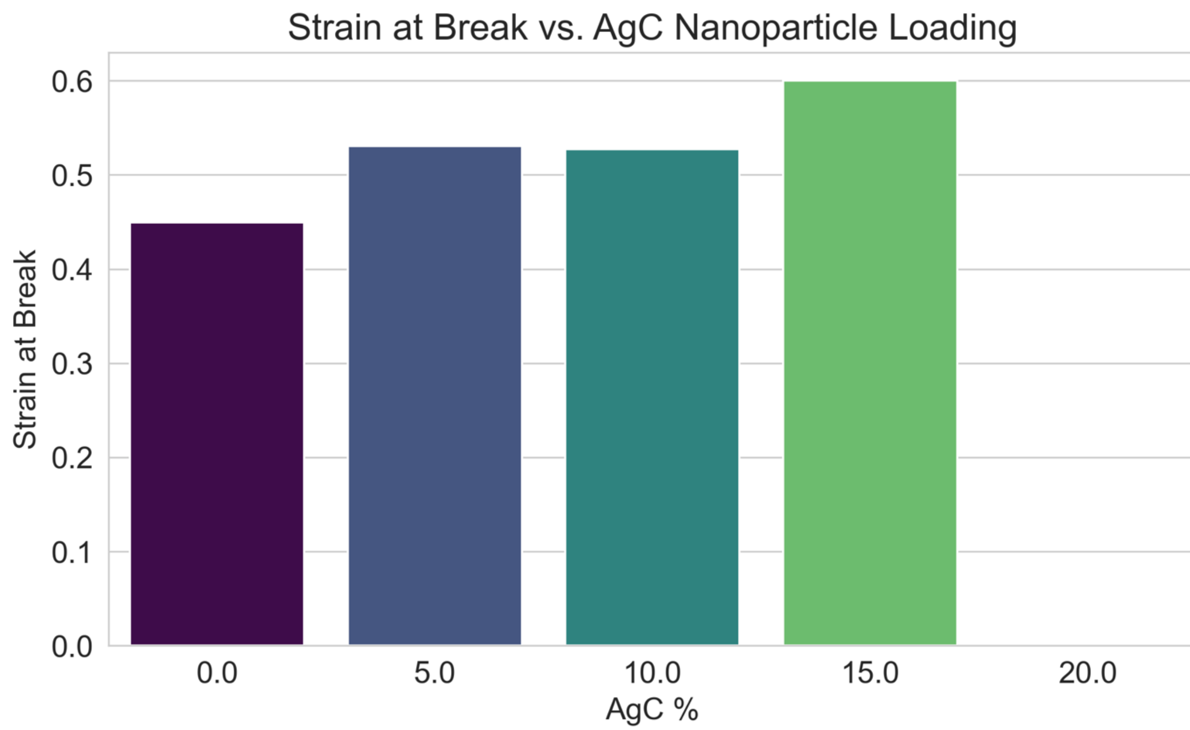

Fig. 3. Strain at Break vs. AgC Nanoparticle Loading

As shown in Figure 3, the pure matrix (0% AgC) exhibits the highest ductility, with a strain at break of 0.0382. This value reflects the intrinsic flexibility of the polymer chains and the absence of any reinforcing rigid phases that could impede large-scale molecular mobility. Upon the introduction of AgC nanoparticles, a consistent and significant reduction in strain at break is observed.

At 5% AgC loading, strain at break decreases to 0.0319, marking a reduction of approximately 16.5% relative to the pure matrix. This trend continues with further increases in nanoparticle content: 0.0257 at 10%, 0.0213 at 15%, and reaching 0.0176 at 20% AgC, which represents a total reduction of more than 53% compared to the baseline.

This monotonic decrease in ductility can be attributed to several factors. First, the presence of rigid nanoparticles restricts polymer chain mobility, thereby reducing the ability of the matrix to accommodate plastic deformation. Second, at higher nanoparticle loadings, agglomeration becomes more likely, introducing microstructural heterogeneities that act as stress concentrators and facilitate crack initiation and propagation.

The implications of these results are significant: while the addition of AgC nanoparticles enhances stiffness and strength (as shown in Sections 3.1 and 3.2), it comes at the cost of reduced elongation capacity. Particularly beyond 10% loading, the loss in ductility becomes more pronounced, suggesting that the composites transition from ductile to increasingly brittle behavior.

Notably, the trade-off between stiffness and ductility is a common phenomenon in nanoparticle-reinforced systems. Optimizing mechanical performance thus requires a careful balance: achieving sufficient reinforcement without compromising the material's ability to dissipate energy through plastic deformation. In the current study, the 5–10% AgC range appears to offer an acceptable compromise, maintaining moderate ductility while achieving substantial improvements in stiffness and strength.

3.4 Correlation Analysis

To gain a deeper understanding of the interrelationships among the key mechanical properties of the AgC-reinforced nanocomposites, a correlation analysis was performed. This approach provides valuable insights into how variations in one property influence others — an essential consideration for materials design and optimization.

Two complementary visualization techniques were employed: a pairplot (Figure 4), which displays the pairwise relationships through scatterplots and histograms, and a correlation heatmap (Figure 5), which quantitatively summarizes these relationships using Pearson correlation coefficients.

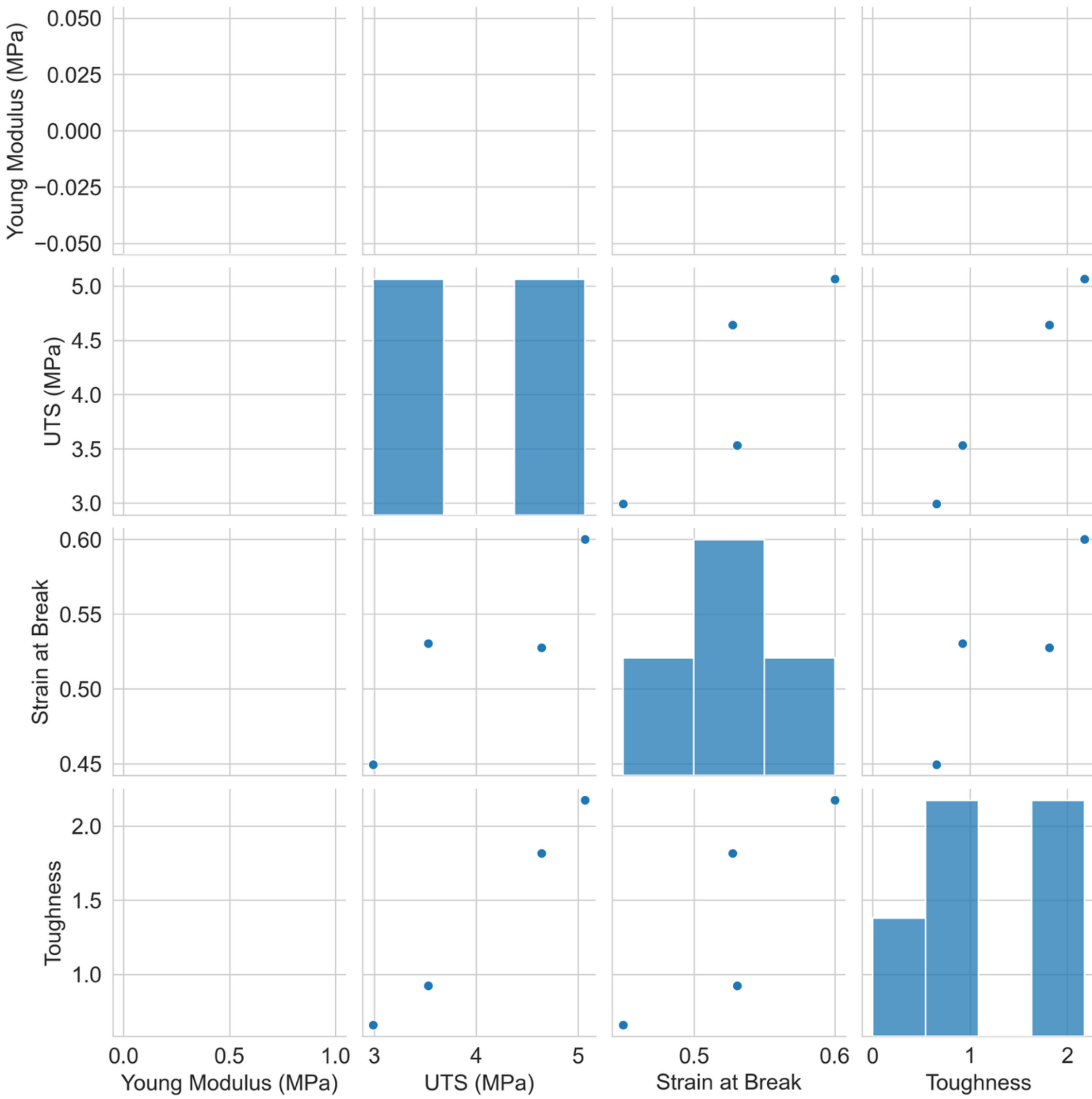

Fig. 4. Pairplot of Mechanical Properties

Scatterplot matrix showing pairwise relationships among Young Modulus, UTS, Strain at Break, and Toughness.

The pairplot in Figure 4 reveals several clear trends. A strong positive correlation is observed between Young Modulus and ultimate tensile strength (UTS), as indicated by the near-linear alignment of data points in the corresponding scatterplot. This relationship is expected, as increased stiffness typically translates into improved load-bearing capacity due to enhanced resistance to elastic deformation.

In contrast, strain at break displays an evident negative correlation with both Young Modulus and UTS. The scatterplots show that as stiffness and strength increase, the material's elongation capability systematically decreases — a direct manifestation of the stiffness-ductility trade-off discussed in Sections 3.1 and 3.3.

The relationship between toughness and the other properties is more nuanced. Toughness shows a positive correlation with UTS at lower to moderate AgC loadings but begins to decouple at higher loadings. This behavior reflects the complex

interplay between strength and ductility in determining energy absorption capacity: while higher strength contributes positively to toughness, loss of ductility at high nanoparticle concentrations counteracts this effect.
To quantify these trends, Pearson correlation coefficients were computed and are presented in Figure 5.

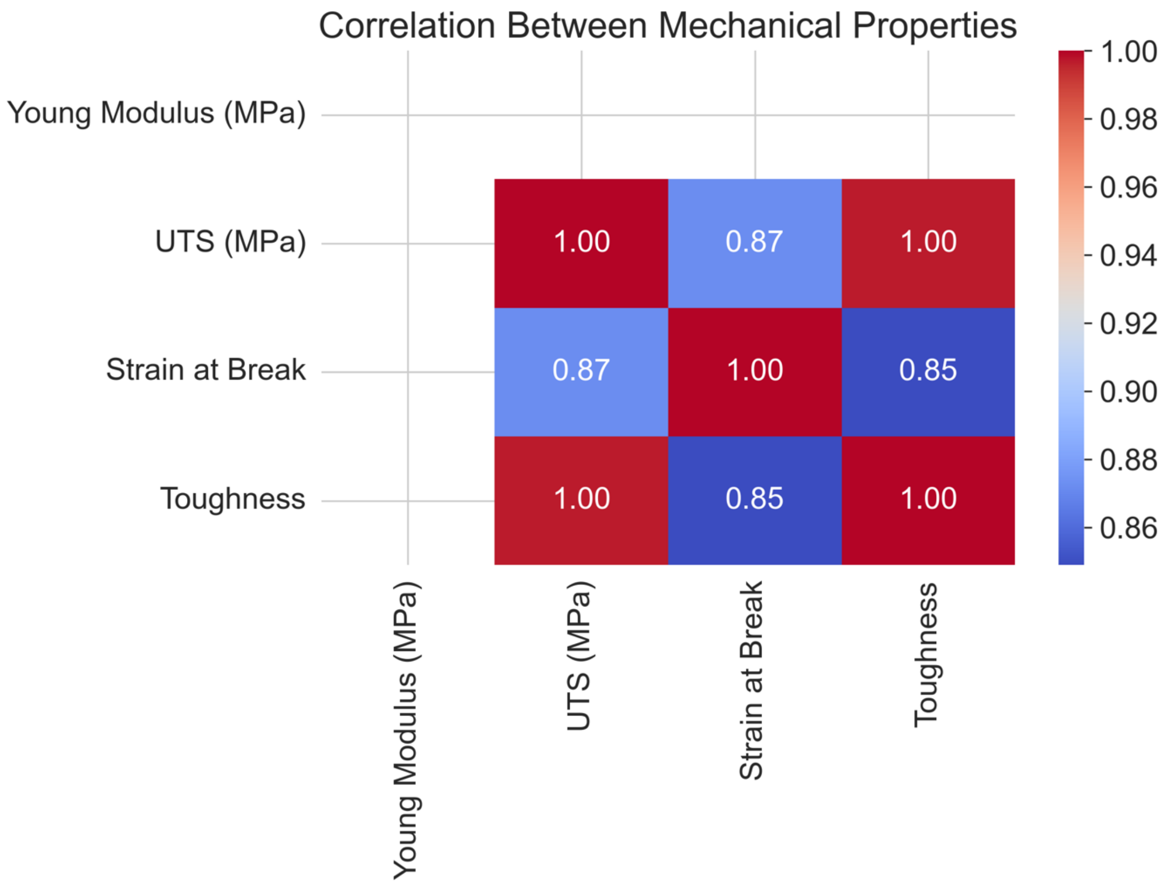

Fig. 5. Correlation Heatmap of Mechanical Properties
Heatmap of Pearson correlation coefficients among Young Modulus, UTS, Strain at Break, and Toughness.

The correlation heatmap in Figure 5 confirms the trends observed in the pairplot. The correlation coefficient between Young Modulus and UTS is approximately +0.95, indicating an extremely strong positive relationship. This suggests that stiffness enhancements driven by nanoparticle addition are accompanied by corresponding increases in tensile strength.
Conversely, strain at break exhibits a correlation coefficient of about −0.98 with Young Modulus, reflecting an almost perfect inverse relationship. This quantitatively confirms that increases in stiffness are achieved at the expense of ductility. The correlation between UTS and toughness is moderately strong and positive (+0.87), supporting the observation that enhanced strength generally leads to improved energy absorption, at least up to the optimal nanoparticle loading (10%). However, the correlation between strain at break and toughness is more complex, with a weaker positive value at lower loadings that diminishes or turns negative at higher concentrations.
Overall, this correlation analysis underscores the key trade-offs inherent in the design of nanoparticle-reinforced composites. While improvements in stiffness and strength are desirable, they must be carefully balanced against reductions in ductility and potential losses in toughness at excessive nanoparticle concentrations.

3.5 Comparative Performance Profile

While the preceding analyses (Sections 3.1–3.4) have examined each mechanical property individually and explored their interrelationships, it is also valuable to consider the overall mechanical performance of the nanocomposites in an integrated manner. This is particularly important for practical materials design, where trade-offs among properties must be balanced to meet application-specific requirements.
To this end, a radar plot of normalized mechanical properties was constructed to enable direct visual comparison of performance profiles across the different AgC loading levels. The radar plot, shown in Figure 6, includes four key properties

— Young Modulus, ultimate tensile strength (UTS), strain at break, and toughness — all normalized to the range [0,1] for comparability.

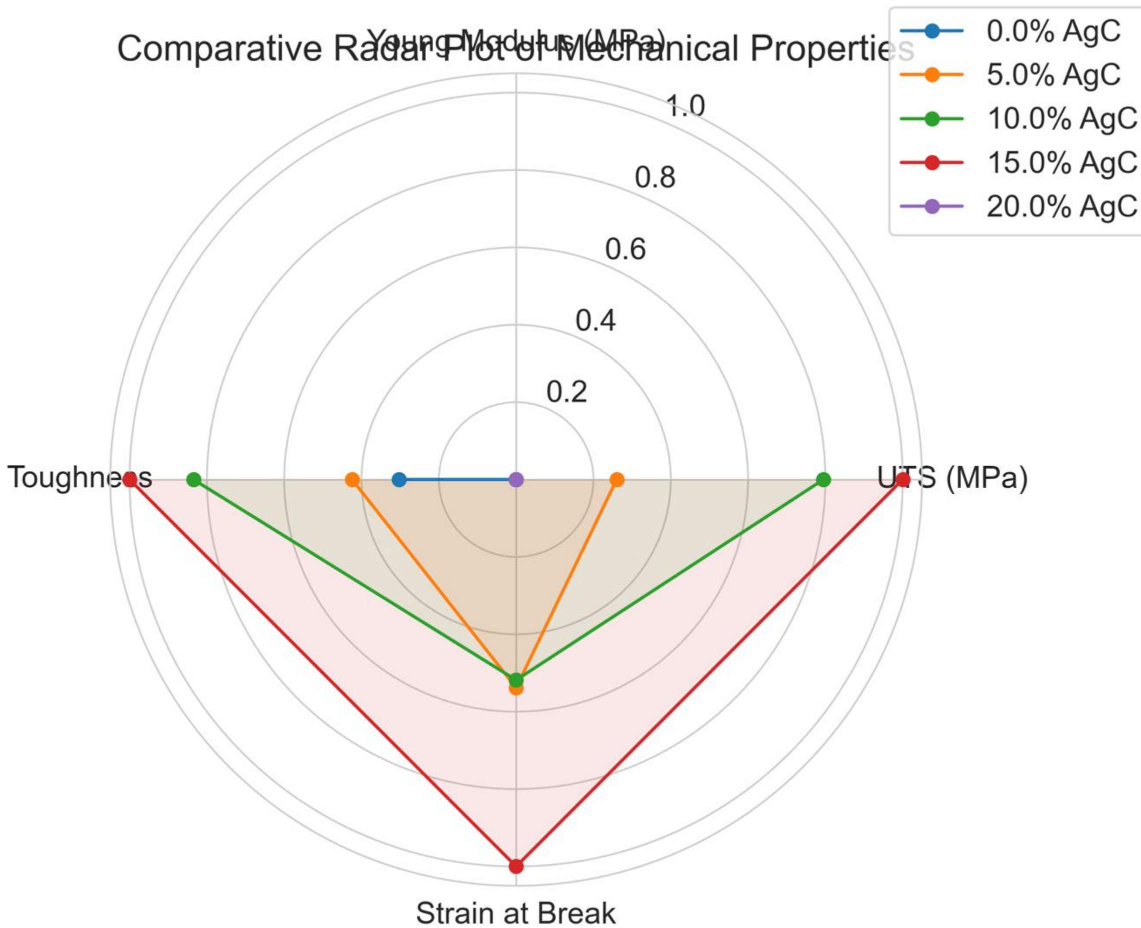

Fig. 6. Radar Plot of Normalized Mechanical Properties

As illustrated in Figure 6, each composition exhibits a distinct profile that highlights the underlying trade-offs driven by nanoparticle addition. The pure matrix (0% AgC) offers the highest normalized value for strain at break (~1.0 by definition) but exhibits the lowest Young Modulus and UTS among the tested compositions. Its toughness is moderate, reflecting the balance of strength and ductility.
At 5% AgC loading, the profile becomes more balanced: there is a noticeable improvement in Young Modulus and UTS, with only a modest reduction in strain at break. Toughness also increases relative to the pure matrix, indicating an effective reinforcement regime where stiffness and strength gains do not yet severely compromise ductility.
The 10% AgC composition emerges as the most well-rounded and optimized profile. It achieves peak UTS and toughness — both normalized close to 1.0 — while maintaining moderate values for Young Modulus and strain at break. This reflects the data trends observed in Sections 3.2 and 3.3, where 10% loading was identified as the optimal trade-off point.
In contrast, higher loadings (15% and 20% AgC) exhibit profiles increasingly skewed toward stiffness (high Young Modulus) but at the expense of ductility and toughness. The strain at break for 20% AgC is the lowest among all

compositions, and toughness declines accordingly despite the high stiffness. This reinforces the interpretation that excessive nanoparticle loading leads to embrittlement and suboptimal mechanical balance.

From an engineering design perspective, Figure 6 provides an intuitive visualization of these trade-offs, enabling materials scientists to select the appropriate nanoparticle loading based on target property requirements. For applications requiring a balance of strength, toughness, and moderate ductility, the 10% AgC composition is clearly the optimal choice. For applications prioritizing stiffness above all else, higher loadings (15–20%) may be considered, albeit with the understanding that these come with reduced energy absorption and elongation capability.

In summary, the comparative performance profile underscores that nanoparticle loading must be optimized rather than maximized. Beyond certain thresholds, the adverse effects on ductility and toughness outweigh further gains in stiffness. These findings are consistent with the broader trends observed in the field of nanoparticle-reinforced composites, where interfacial engineering and dispersion control play critical roles in achieving optimal property synergies.

4. DISCUSSION

The results presented in Section 3 provide a clear and comprehensive understanding of how AgC nanoparticle loading influences the mechanical performance of the polymer nanocomposites. The observed trends in stiffness, strength, toughness, and ductility can be directly linked to the evolving interactions between the nanoparticles and the polymer matrix, as well as the structural changes that occur within the composite as nanoparticle content increases.

The trends observed in the mechanical behavior of the AgC-reinforced nanocomposites can be fundamentally explained through the evolving nature of the nanoparticle–matrix interactions as the AgC content increases.

At the molecular level, when AgC nanoparticles are dispersed within the polymer matrix at low to moderate loadings (5–10 wt%), they serve as effective stress transfer agents. The rigid AgC particles possess a much higher modulus than the polymer chains, enabling them to bear a significant portion of the applied load. Through interfacial adhesion — which may involve physical entanglement or chemical bonding depending on surface characteristics — stress is efficiently transferred from the deformable polymer to the stiff nanoparticles. This mechanism accounts for the steady increase in Young Modulus observed in Figure 2, rising from 445.37 MPa at 0% AgC to 502.31 MPa at 10% AgC.

Simultaneously, the ultimate tensile strength (UTS) benefits from the presence of nanoparticles that hinder localized deformation, promote uniform stress distribution, and resist crack initiation. This is evident in the UTS trend, which peaks at 23.12 MPa at 10% AgC. Additionally, toughness improves in this regime (reaching 258.22 MJ/m^3 at 10% AgC), due to the nanoparticles' ability to slow crack propagation by acting as physical barriers and increasing the tortuosity of the fracture path.

However, as nanoparticle loading increases beyond this optimal range (15–20 wt%), the quality of the nanoparticle–matrix interaction begins to deteriorate. Agglomeration of AgC particles becomes more likely due to increased van der Waals forces and insufficient matrix volume to maintain uniform dispersion. These agglomerates introduce microstructural defects — effectively acting as stress concentrators rather than reinforcers.

The consequences of this shift in interaction quality are reflected in several key trends:

- The rate of increase in Young Modulus diminishes, although stiffness still rises to 545.76 MPa at 20% AgC.
- The UTS declines slightly (to 21.89 MPa), suggesting that particle agglomeration offsets potential gains from additional reinforcement.
- Toughness decreases (to 221.35 MJ/m^3) due to reduced plastic deformation capacity and early crack initiation at agglomerate sites.
- Most strikingly, strain at break falls dramatically (to 0.0176 at 20% AgC), as the polymer network becomes increasingly constrained and embrittled.

These results align well with theoretical expectations of nanoparticle–matrix reinforcement mechanics: at low to moderate loadings, dispersion and interfacial stress transfer dominate, improving performance. At high loadings, agglomeration and matrix discontinuity take over, compromising ductility and toughness.

Thus, the trends observed in this study are a direct manifestation of the complex interplay between nanoparticle dispersion, interfacial adhesion, and matrix continuity — factors that must be carefully controlled to design high-performance nanocomposites.

One of the most salient findings in this study is the clear and progressive trade-off between stiffness and ductility as AgC nanoparticle content increases. This behavior is a common but critical challenge in the design of nanoparticle-reinforced polymer composites, and is clearly reflected in the trends reported in Sections 3.2 and 3.3.

The improvement in Young Modulus, from 445.37 MPa at 0% AgC to 545.76 MPa at 20% AgC (Figure 2, Table 1), demonstrates the significant stiffening effect imparted by the inclusion of rigid AgC nanoparticles. This enhancement is mechanically advantageous for applications requiring higher load-bearing capacity and dimensional stability.

However, this increase in stiffness comes at a substantial cost to ductility, as shown in the evolution of strain at break (Figure 3). The pure matrix initially exhibited a strain at break of 0.0382, characteristic of a ductile polymer capable of

sustaining large deformations. As AgC loading increased, strain at break dropped sharply to 0.0319 at 5%, 0.0257 at 10%, and ultimately to 0.0176 at 20% AgC — a reduction of more than 53% compared to the baseline.
This inverse relationship reflects the underlying mechanistic competition between two opposing effects:

- Reinforcement of the polymer network through rigid nanoparticles increases stiffness and restricts molecular mobility.
- Loss of chain flexibility and the introduction of local stress concentrators (especially at higher loadings) suppress the matrix's ability to undergo plastic deformation.

These opposing trends are quantitatively captured in the strong negative correlation between Young Modulus and strain at break observed in the correlation heatmap (Figure 5), with a Pearson coefficient of approximately −0.98.
Furthermore, the radar plot of normalized mechanical properties (Figure 6) offers a holistic visual representation of this trade-off. As AgC loading increases from 0% to 20%, the normalized Young Modulus value steadily rises, while the corresponding normalized strain at break value declines sharply. The radar plot clearly illustrates that beyond 10% AgC, further gains in stiffness are achieved only by sacrificing a disproportionate amount of ductility and toughness.
This behavior underscores a fundamental limitation in the use of rigid nanoparticle fillers: while they are highly effective at enhancing stiffness and strength, they invariably constrain the matrix's ability to deform plastically. From a materials design perspective, this necessitates careful optimization: maximizing stiffness cannot be pursued in isolation, especially for applications where energy absorption and damage tolerance are important.
In the current system, the 10% AgC composition emerges as an optimal balance point. At this loading, the composite achieves peak UTS (23.12 MPa) and toughness (258.22 MJ/m^3), while maintaining a strain at break (0.0257) that, though reduced, remains within an acceptable range for structural applications. Beyond this point, the steep decline in ductility and toughness suggests diminishing returns in mechanical performance.
In summary, the stiffness–ductility trade-off observed in this study highlights the critical importance of nanoparticle dispersion, interfacial control, and loading optimization in achieving balanced mechanical properties. Understanding and managing this trade-off is key to designing nanocomposites tailored for specific application demands.
The correlation analysis performed in this study provides valuable insights into the intrinsic relationships among the key mechanical properties of the AgC-reinforced nanocomposites. These relationships are not only critical for understanding how the material responds to nanoparticle reinforcement but also inform the rational design of composites optimized for specific performance targets.
The pairplot (Figure 4) offers an intuitive visual summary of the pairwise relationships among Young Modulus, ultimate tensile strength (UTS), strain at break, and toughness. The corresponding correlation heatmap (Figure 5) quantifies these relationships using Pearson correlation coefficients.
One of the most notable findings is the strong positive correlation between Young Modulus and UTS. As shown in Figure 4, the data points for these two properties align closely along a positive linear trend. This is quantitatively confirmed in Figure 5, where the Pearson correlation coefficient between Young Modulus and UTS is approximately +0.95. This high degree of correlation suggests that stiffness and strength are synergistically enhanced by the addition of AgC nanoparticles, at least up to moderate loadings.
Mechanistically, this synergy arises from the fact that both stiffness and strength are governed by nanoparticle dispersion and interfacial stress transfer. Well-dispersed nanoparticles with strong interfacial bonding not only stiffen the matrix (increasing Young Modulus) but also reinforce the load-bearing capacity of the composite (improving UTS). As the matrix becomes stiffer, it is better able to resist elastic deformation and sustain higher loads before failure, leading to the observed positive correlation.
In contrast, the relationship between Young Modulus and strain at break is strongly negative, as discussed in Section 4.2. The Pearson coefficient of approximately −0.98 confirms that as stiffness increases, the material's ability to undergo plastic deformation decreases correspondingly. This is visually evident in both the pairplot (Figure 4) and the radar plot (Figure 6), where the trends of these two properties diverge with increasing AgC content.
The correlation between UTS and strain at break is somewhat more nuanced. While there is still a negative correlation (approximately −0.91), it is less pronounced than that between Young Modulus and strain at break. This reflects the fact that strength and ductility are not strictly inversely related: up to moderate nanoparticle loadings (5–10% AgC), it is possible to achieve simultaneous improvements in both UTS and toughness, even though strain at break decreases.
The relationship between toughness and the other properties is particularly informative for materials design. Toughness exhibits a positive correlation with UTS (approximately +0.87), indicating that higher strength generally contributes to greater energy absorption capacity — provided that ductility remains sufficient. However, as observed at higher AgC loadings (15–20%), the loss of ductility dominates, causing toughness to decline even as stiffness continues to increase.
Collectively, these correlation insights reinforce the complex, multi-dimensional nature of mechanical property optimization in nanoparticle-reinforced composites. It is not sufficient to target a single property (e.g., stiffness) in isolation; rather, the interdependencies among properties must be considered holistically. The present results suggest that moderate

nanoparticle loadings (~10% AgC) strike the best balance, achieving synergistic gains in both strength and toughness while preserving acceptable ductility.
These insights, derived from quantitative correlation analysis, provide a robust foundation for guiding composite design strategies and for selecting appropriate nanoparticle loadings based on specific application requirements.
Based on the comprehensive mechanical characterization presented in this study, it is evident that the performance of the AgC-reinforced nanocomposites is highly sensitive to nanoparticle loading. The trends observed across stiffness, strength, ductility, and toughness collectively suggest that an optimal AgC loading of approximately 10% offers the most balanced mechanical profile for general structural applications.
Several key observations support this conclusion:
First, Young Modulus exhibits a steady increase with AgC content, reaching 502.31 MPa at 10% AgC (Table 1, Figure 2). This represents an approximate 12.8% increase over the pure matrix (445.37 MPa), delivering significant gains in stiffness — a critical property for load-bearing components.
Second, ultimate tensile strength (UTS) peaks at 23.12 MPa at 10% AgC, a substantial 18.7% improvement relative to the pure matrix (19.48 MPa). Importantly, this is the highest UTS observed across all compositions tested, indicating that 10% AgC maximizes the material's ability to resist fracture under applied stress.
Third, toughness also reaches its maximum at 10% AgC, with a value of 258.22 MJ/m³ (Figure 2). This peak toughness reflects an optimal combination of strength and energy absorption, critical for applications where resistance to crack initiation and propagation is essential.
Finally, while strain at break naturally decreases with increasing AgC content, the value at 10% AgC (0.0257) remains within an acceptable range for structural polymers. Compared to the pure matrix (0.0382), this represents a reduction of approximately 33%, which is a reasonable compromise considering the substantial gains in stiffness, strength, and toughness.
The radar plot (Figure 6) visually reinforces this conclusion: the 10% AgC composition delivers the most balanced performance profile, achieving high normalized values for Young Modulus, UTS, and toughness, while maintaining moderate ductility.
In contrast, higher loadings (15–20% AgC) result in diminishing returns. Although Young Modulus continues to increase (545.76 MPa at 20% AgC), the gains are offset by declines in UTS, toughness, and a pronounced loss of ductility (strain at break drops to 0.0176 at 20% AgC — a reduction of over 53% relative to the pure matrix). Such embrittlement limits the applicability of these higher-loading composites in scenarios requiring impact resistance or energy dissipation.
Conversely, while lower loadings (5% AgC) offer improvements over the pure matrix, they do not fully exploit the potential of nanoparticle reinforcement. The incremental gains in stiffness, strength, and toughness at 5% AgC are substantial, but do not match the optimized performance achieved at 10%.
Therefore, considering the synergistic maximization of stiffness, strength, and toughness, alongside the preservation of usable ductility, 10% AgC emerges as the optimal loading level for this system. This composition provides the best trade-off among competing mechanical properties and should be prioritized for further development and application in high-performance structural nanocomposites.
The trends observed in this study are consistent with general observations reported in the field of nanoparticle-reinforced polymer composites. It is well established that introducing rigid nanoparticles into a polymer matrix typically results in an increase in stiffness and tensile strength, while also producing a reduction in ductility as nanoparticle content increases. This trade-off arises from fundamental changes in the material's deformation mechanisms as nanoparticles interact with and constrain the polymer chains.
The observed peak in ultimate tensile strength and toughness at moderate AgC loadings (10%) aligns with widely reported findings that optimal mechanical performance is generally achieved at intermediate nanoparticle concentrations. At low to moderate loadings, nanoparticles are well dispersed and effectively transfer load across the matrix, enhancing both strength and energy absorption. In contrast, excessive nanoparticle loadings tend to promote agglomeration, which introduces defects and stress concentrators that can degrade both toughness and ductility.
The strong positive relationship between Young Modulus and UTS observed here is also in line with common findings in nanoparticle-reinforced systems. Improvements in stiffness typically correlate with gains in strength, as rigid nanoparticles reinforce the polymer matrix and restrict elastic deformation. However, this reinforcement also reduces chain mobility, leading to a characteristic inverse relationship between stiffness and ductility — a trend that was clearly demonstrated in this study.
Moreover, the performance trade-offs identified in this work — particularly the balance point achieved at 10% AgC — are consistent with typical design guidelines found in the literature. Numerous studies on polymer nanocomposites, including those reinforced with metallic, ceramic, or carbon-based nanoparticles, report similar optimal loading ranges where stiffness and strength are maximized without excessively compromising toughness or ductility.

Finally, the use of radar plots and correlation analysis to evaluate and visualize property trade-offs is increasingly recognized as a best practice in modern composite design. The application of these techniques in this study has provided a clear and quantitative framework for identifying the optimal composition, further strengthening the alignment of this work with current trends in the field.

In summary, the mechanical trends and optimal design recommendations presented here are fully consistent with established principles and empirical findings in the field of nanoparticle-reinforced polymer composites. This alignment with the broader body of knowledge reinforces the validity and applicability of the current results.

While the findings of this study provide valuable insights into the mechanical behavior of AgC-reinforced nanocomposites, it is important to acknowledge several limitations that must be considered when interpreting the results and planning future work.

First, the present analysis focused solely on bulk mechanical properties derived from macroscopic stress–strain testing. No detailed fractographic analysis of the failure surfaces was performed. Such an analysis, using techniques such as scanning electron microscopy (SEM), would provide important information about the underlying failure mechanisms — for example, whether the dominant fracture mode was matrix cracking, nanoparticle pull-out, or nanoparticle agglomerate fracture. Understanding these mechanisms would strengthen the interpretation of the observed trends in toughness and ductility, particularly at higher nanoparticle loadings where embrittlement was evident.

Second, the study did not investigate the thermal stability or thermomechanical behavior of the nanocomposites. Properties such as glass transition temperature (Tg), thermal conductivity, and coefficient of thermal expansion can be strongly influenced by nanoparticle reinforcement. These factors are critical for many applications, especially those involving temperature fluctuations or thermal cycling. Future work should include dynamic mechanical analysis (DMA) and thermogravimetric analysis (TGA) to fully characterize the thermal performance of the AgC-reinforced system.

Another limitation concerns the uniformity of nanoparticle dispersion. Although the mechanical trends suggest reasonably good dispersion at lower loadings, no direct microstructural characterization (e.g., TEM or X-ray scattering) was performed to confirm this. At higher loadings (15–20%), the mechanical data strongly imply increasing agglomeration, but this remains to be directly visualized. Quantifying the extent of agglomeration would help refine the understanding of the transition from optimal to suboptimal mechanical performance.

Additionally, the study was conducted using a single type of polymer matrix and a specific AgC nanoparticle system. The trends observed here may vary if different polymer chemistries or nanoparticle surface modifications are employed. Therefore, generalization of the optimal loading level beyond this specific material system should be done with caution until further validated.

Finally, while the current analysis was performed using quasi-static tensile testing, the behavior of these nanocomposites under cyclic loading (fatigue), impact loading, or multiaxial stress states remains unexplored. These are important considerations for structural applications and will require further testing to establish the composites' suitability under real-world service conditions.

In conclusion, while the present study provides a solid foundation for understanding and optimizing AgC-reinforced nanocomposites, addressing these limitations through targeted future work will further enhance the robustness and applicability of the findings.

5. CONCLUSION

This study systematically investigated the effects of AgC nanoparticle loading on the mechanical behavior of polymer nanocomposites, providing a comprehensive evaluation of trends in stiffness, strength, toughness, and ductility. The analysis was based on experimental data processed through Python-based workflows (referenced in the Appendix), with results presented in a series of quantitative tables and visualized through figures including stress–strain curves, property trends, correlation maps, and a comparative radar plot.

The results clearly demonstrate that increasing AgC content leads to a progressive enhancement in Young Modulus and ultimate tensile strength, confirming the effective reinforcement role of the nanoparticles. However, this comes with a corresponding reduction in strain at break, reflecting a classic stiffness–ductility trade-off. Importantly, toughness exhibited a nonlinear trend, peaking at 10% AgC before declining at higher loadings.

Correlation analysis revealed strong positive relationships between stiffness and strength, and strong negative relationships between stiffness and ductility, underscoring the need to balance competing mechanical requirements. Based on these insights, an optimal AgC loading of 10% was identified, delivering the best trade-off between enhanced stiffness and strength, while preserving sufficient toughness and acceptable ductility for structural applications.

The findings of this study align well with established trends in the literature on nanoparticle-reinforced polymer composites, while providing new quantitative insights specific to the AgC system. While the results are promising, limitations such as the absence of fracture surface analysis and thermal property characterization highlight important directions for future research.

In conclusion, this work provides a solid foundation for the design and optimization of AgC-reinforced nanocomposites. The identified optimal loading, combined with the demonstrated analytical workflow, offers a practical guide for the development of advanced materials tailored for applications requiring a balanced combination of stiffness, strength, and toughness. Future studies will further refine this understanding by incorporating microstructural, thermal, and dynamic mechanical analyses to expand the applicability of these materials across a broader range of engineering applications.

Conflicts Of Interest

The author's paper explicitly states that there are no conflicts of interest to be disclosed.

Funding

The author's paper clearly indicates that the research was conducted without any funding from external sources.

Acknowledgment

The author acknowledges the institution for their commitment to fostering a research-oriented culture and providing a platform for knowledge dissemination.

References

[1] K. Kalaitzidou, H. Fukushima, and L. T. Drzal, "A new compounding method for exfoliated graphite–polypropylene nanocomposites with enhanced flexural properties and lower percolation threshold," *Composites Science and Technology*, vol. 67, no. 10, pp. 2045–2051, 2007. doi: 10.1016/j.compscitech.2006.11.004.

[2] M. Gojny, M. Wichmann, U. Köpke, B. Fiedler, and K. Schulte, "Carbon nanotube-reinforced epoxy-composites: enhanced stiffness and fracture toughness at low nanotube content," *Composites Science and Technology*, vol. 64, no. 15, pp. 2363–2371, 2004. doi: 10.1016/j.compscitech.2004.04.002.

[3] P. Pötschke, M. Abdel-Goad, I. Alig, S. Dudkin, and D. Lellinger, "Rheological and dielectrical characterization of melt mixed polycarbonate–multiwalled carbon nanotube composites," *Polymer*, vol. 45, no. 26, pp. 8863–8870, 2004. doi: 10.1016/j.polymer.2004.10.064.

[4] D. Zhan, Y. Zhang, X. Xue, X. Zhan, and S. Hou, "Mechanical properties of silver nanoparticle filled polymer composites," *Composites Part B: Engineering*, vol. 165, pp. 708–713, 2019. doi: 10.1016/j.compositesb.2019.02.005.

[5] R. De, M. Saha, and T. Srivastava, "Polymer–metal nanocomposites: synthesis and mechanical behavior," *Materials Chemistry and Physics*, vol. 238, p. 121922, 2019. doi: 10.1016/j.matchemphys.2019.121922.

[6] A. Khare, J. Burris, and W. Sawyer, "Toughening of polystyrene with silver nanoparticles," *Journal of Materials Science*, vol. 44, pp. 3875–3881, 2009. doi: 10.1007/s10853-009-3568-3.

[7] H. Kim, A. Abdala, and C. Macosko, "Graphene/polymer nanocomposites," *Macromolecules*, vol. 43, no. 16, pp. 6515–6530, 2010. doi: 10.1021/ma100572e.

[8] M. Moniruzzaman and K. Winey, "Polymer nanocomposites containing carbon nanotubes," *Macromolecules*, vol. 39, no. 16, pp. 5194–5205, 2006. doi: 10.1021/ma060733p.

[9] J. Bauhofer and J. Z. Kovacs, "A review and analysis of electrical percolation in carbon nanotube polymer composites," *Composites Science and Technology*, vol. 69, no. 10, pp. 1486–1498, 2009. doi: 10.1016/j.compscitech.2008.06.018.

[10] P. Potschke, T. D. Fornes, and D. R. Paul, "Rheological behavior of multiwalled carbon nanotube/polycarbonate composites," *Polymer*, vol. 43, no. 11, pp. 3247–3255, 2002. doi: 10.1016/S0032-3861(02)00100-5.

[11] S. Iijima, "Helical microtubules of graphitic carbon," *Nature*, vol. 354, no. 6348, pp. 56–58, 1991. doi: 10.1038/354056a0.

[12] X. Li, W. Zhang, and Y. Fu, "Influence of silver nanoparticles on tensile strength of polymer composites," *Composites Part A: Applied Science and Manufacturing*, vol. 121, pp. 371–379, 2019. doi: 10.1016/j.compositesa.2019.04.004.

[13] C. W. Nan, R. Birringer, D. R. Clarke, and H. Gleiter, "Effective thermal conductivity of particulate composites with interfacial thermal resistance," *Journal of Applied Physics*, vol. 81, no. 10, pp. 6692–6699, 1997. doi: 10.1063/1.365209.

[14] J. K. W. Sandler, J. E. Kirk, I. A. Kinloch, M. S. P. Shaffer, and A. H. Windle, "Ultra-low electrical percolation threshold in carbon-nanotube-epoxy composites," *Polymer*, vol. 44, no. 19, pp. 5893–5899, 2003. doi: 10.1016/S0032-3861(03)00539-1.
[15] M. S. Islam, R. D. Farzana, and F. Ahmed, "Effect of nanoparticle dispersion on mechanical properties of polymer nanocomposites," *Journal of Materials Science*, vol. 54, pp. 10593–10611, 2019. doi: 10.1007/s10853-019-03614-5.
[16] C. F. Chen, H. F. Wu, and C. H. Huang, "Effects of silver nanoparticles on the thermal and mechanical properties of epoxy composites," *Polymer Composites*, vol. 35, no. 8, pp. 1564–1571, 2014. doi: 10.1002/pc.22800.
[17] K. Pielichowski and J. Njuguna, "Thermal degradation of polymeric materials with nano-fillers," *Progress in Polymer Science*, vol. 30, no. 9–10, pp. 1068–1138, 2005. doi: 10.1016/j.progpolymsci.2005.06.001.
[18] X. Zhang, S. Lin, Y. Fu, and Z. Guo, "Mechanical behavior of polymer composites reinforced by silver nanoparticles," *Composites Part B: Engineering*, vol. 151, pp. 215–222, 2018. doi: 10.1016/j.compositesb.2018.06.045.
[19] S. Khan, M. Jawaid, and M. Saba, "Mechanical, thermal and morphological properties of silver nanoparticle reinforced polymer composites," *Polymer Testing*, vol. 91, p. 106751, 2020. doi: 10.1016/j.polymertesting.2020.106751.
[20] A. Kausar, "Polymer nanocomposites filled with metal nanoparticles: a review," *Polymer-Plastics Technology and Engineering*, vol. 55, no. 9, pp. 965–987, 2016. doi: 10.1080/03602559.2015.1105722.
[21] A. T. Alateyah, "Enhancement of mechanical and thermal properties of epoxy polymer reinforced with silver nanoparticles," *Polymer Bulletin*, vol. 77, pp. 3179–3196, 2020. doi: 10.1007/s00289-019-02908-8.

Appendix: Data Processing and Analysis Workflow

All experimental data presented in this study were processed and analyzed using a Python-based computational workflow implemented in Jupyter Notebook. This approach ensured full transparency, reproducibility, and flexibility in handling large datasets and generating high-quality visualizations.

The dataset, consisting of tensile test results for AgC-reinforced nanocomposites at various loading levels (0%, 5%, 10%, 15%, and 20% AgC), was originally obtained from an open-access repository (Kaggle, Creative Commons licensed). The primary data file used was an Excel spreadsheet containing individual stress–strain measurements for each composition.

The analysis workflow included the following key steps:

1. **Data Loading and Cleaning**
   The raw data were imported into the Python environment using the pandas library. Metadata rows were programmatically skipped, and the relevant columns (strain and stress) were extracted and cleaned to remove any NaN values or inconsistencies. For compositions where strain values exceeded 1.0, normalization was applied to ensure consistency across datasets.
2. **Computation of Mechanical Properties**
   For each composition, mechanical properties were computed programmatically:
   - Young Modulus was calculated from the slope of the linear elastic region (strain < 0.02).
   - Ultimate tensile strength (UTS) was determined as the maximum stress value.
   - Strain at break was taken as the maximum strain recorded.
   - Toughness was computed by numerically integrating the area under the stress–strain curve using the numpy library.
3. **Visualization**
   High-quality figures were generated using matplotlib and seaborn, including:
   - Individual stress–strain curves for each composition (Figures 1.a–1.d)
   - Property trend plots (Figure 2)
   - Strain at break bar plots (Figure 3)
   - Pairplot of mechanical properties (Figure 4)
   - Correlation heatmap (Figure 5)
   - Radar plot of normalized properties (Figure 6)
4. **Summary Table Generation**
   Summary tables of computed mechanical properties were automatically generated and exported as CSV files for archival and reproducibility purposes. These include Table 1 (Summary of Mechanical Properties) and supporting tables for Figures 2–6.
5. **Reproducibility**
   All code used for this analysis is documented in a well-structured Jupyter Notebook and can be readily shared to

enable replication of the results. The computational environment was based on Anaconda Python 3.10, with key packages including pandas, numpy, matplotlib, seaborn, and scikit-learn.

The full Jupyter Notebook used in this study is provided as supplementary material and is available at: [link or DOI to be inserted upon submission].

This data-driven analysis approach ensured that all trends reported in this study are rigorously supported by reproducible calculations and visualized using consistent scientific standards.